European Journal of Agronomy 96 (2018) 108–119

Contents lists available at ScienceDirect

European Journal of Agronomy

journal homepage: www.elsevier.com/locate/eja

Future climate change projects positive impacts on sugarcane productivity in southern China

Hongyan Ruan[a,b,c], Puyu Feng[b,d], Bin Wang[b], Hongtao Xing[b], Garry J. O'Leary[e], Zhigang Huang[a,c,*], Hao Guo[a,c], De Li Liu[b,f,**]

[a] State Key Laboratory for Conservation and Utilization of Subtropical Agro-Bioresources, Agricultural College, Guangxi University, Nanning 530000, Guangxi, China
[b] NSW Department of Primary Industries, Wagga Wagga Agricultural Institute, Wagga Wagga, NSW 2650, Australia
[c] Cultivation Base of Guangxi Key Laboratory for Agro-Environment and Agro-Product Safety, China
[d] School of Life Sciences, Faculty of Science, University of Technology Sydney, PO Box 123, Broadway, Ultimo, NSW 2007, Australia
[e] Agriculture Victoria Research, Department of Economic Development, Jobs, Transport and Resources, PB 260, Horsham, Vic 3400, Australia
[f] Climate Change Research Centre and ARC Centre of Excellence for Climate Extremes, University of New South Wales, Sydney, NSW, Australia

ARTICLE INFO

Keywords:
APSIM-Sugarcane
Sugarcane yield
Elevated CO_2
Statistical downscaling
General circulation model
High temperature

ABSTRACT

Climate change is recognised to alter the distribution of rainfall and increase temperature and atmospheric CO_2 concentration [CO_2] and pose a formidable challenge to the sustainability of various cropping industries around the world. Additionally, in specific regions, like China, and for particular crops, like sugarcane, the likely effects of climate change are not straightforward. This is because of non-linearity of the interacting climatic factors on crop growth and yield. In our study, the APSIM-Sugarcane model was used to examine the likely response of sugarcane in future climate scenarios. Statistically downscaled climate data based on 28 global climate models (GCMs) under RCP4.5 and RCP8.5 scenarios were used to generate the change in climate in southern China. The results show that the model well reproduced observations for biomass dry matter (DM), biomass fresh matter (FM), sugar yields (S) and leaf area index (LAI), with values for the index of agreement of 0.65, 0.71, 0.84 and 0.70, respectively. The values of RMSE were relatively low with 7.10 t ha^{-1} for DM, 18.87 t ha^{-1} for FM, 0.84 t ha^{-1} for S and 1.03 m^2 m^{-2} for LAI. On average, the ensemble of downscaled GCM projections showed a small increase in radiation and rainfall in the future at the four locations considered, with significantly increased temperature. Sugarcane yields in southern China appeared to be positively affected under future climate and [CO_2] changes. Overall, DM was projected to increase by 5.6 and 6.4 and 6.6 t ha^{-1} for RCP4.5 in 2030s, 2060s and 2090s relative to 1961–2010, respectively. However, RCP8.5 had less promotion compared to RCP4.5 on DM. Similar increased trends for three future time periods could be found in FM and S. Our results showed that the largest percentage change in S occurred at high latitude locations (e.g., Hezhou), with mean values 28.1% and 39.4% for RCP4.5 and RCP8.5 in 2030s, 44.2% and 23.5% in 2060s, and 41.1% and 45.5% for in 2090s, respectively. In addition, our multiple linear regression analyses showed that the changes in radiation, rainfall and temperature together with elevated [CO_2] could explain more than 70% of sugarcane yields change across four locations. Across all locations, increases in sugarcane yields were strongly correlated (P = .001) with each degree (Celsius) increase in future temperature and per mm increase in future rainfall. For example, the DM, FM and S increased 7.8–14.2, 16.6–36.1 and 2.7–6.1 kg ha^{-1} mm^{-1} responding to rainfall, respectively. Although uncertainties in our study on the impact of climate change on sugarcane might arise from the choice of crop model and GCMs, the results would be pivotal for developing high-yield adaptive strategies as well as informing policy makers to improve sugarcane productivity in China.

1. Introduction

Sugarcane is a perennial grass grown over a wide range of climates around the world from latitudes of 30°N to 30°S (Bull and Glasziou, 1979). The crop is usually cultivated in the tropical and sub-tropical regions with adequate solar radiation and rainfall. The Chinese sugar

* Corresponding author at: State Key Laboratory for Conservation and Utilization of Subtropical Agro-Bioresources, Agricultural College, Guangxi University, Nanning 530000, Guangxi, China.
** Corresponding author at: NSW Department of Primary Industries, Wagga Wagga Agricultural Institute, Wagga Wagga, NSW 2650, Australia.
E-mail addresses: hzg@gxu.edu.cn (Z. Huang), de.li.liu@dpi.nsw.gov.au (D.L. Liu).

https://doi.org/10.1016/j.eja.2018.03.007
Received 21 September 2017; Received in revised form 9 February 2018; Accepted 24 March 2018
Available online 06 April 2018
1161-0301/ © 2018 Elsevier B.V. All rights reserved.

industry is mainly located in the southern part of China that comprise mainly C4 sugarcane crops (*Saccharum* ssp.) and is about 1.5 million ha in size (Li and Yang, 2015). In contrast, only 14% of Chinese sugar production comes from sugar beet (*Beta vugalis* L.) that is grown in the cooler elevated northern regions (Huang et al., 2006). Guangxi has the largest sugarcane area and is the largest producer of sugar in China, accounting for about 70% of national area producing 7.21 million tons sugar per annum, which contributes to about 7 billion US dollars to the Gross Domestic Product (Li and Yang, 2015). This makes sugar a vital industry in Guangxi and for China generally (Zhu et al., 2007).

Rainfall, temperature and radiation are the major climate factors that affect sugarcane growth and development. Compared to the production of other sugar producing regions of the world, the long duration of low temperature, frost occurrence, wet and cloudy days in winter and spring are the major environmental factors that lead to severe constraints for sugarcane growth, especially for ratoon sprouting and the maturing period of accumulating sucrose and juice purity (Li et al., 2015). In addition, drought occurs often in the major sugarcane areas, which is also a major constraint because more than 80% of sugarcane is planted in the upland areas where irrigation is not available (Li and Yang, 2015).

Clearly, developing strategies to cope with the negative or take advantage of positive impacts of climate change is essential to inform public debate, policy makers and farmers to maintain sugar production in China. Increasing greenhouse gas concentrations are expected to increase China's surface air temperature and alter the temporal and spatial patterns of rainfall. The annual mean air temperature is predicted to increase 2.3–3.3 °C by 2050 and 3.9–6.0 °C by 2100, and annual rainfall is projected to increase 10–12% in 2100 relative to the 30-year average of 1961–1990 in China (Ding et al., 2006). Inevitably, future climate change would have significant impacts for sugarcane productivity. Therefore, sufficiently accurate predictions of sugarcane response to climate change are necessary to inform successful adaptation.

However, the effect of the interaction between rising CO_2 concentration [CO_2], increased temperature and rainfall on sugarcane yield has not been documented in this region, though there are many studies in the major sugar production regions in the world, that has assessed the effect of climate change on sugarcane yield (Biggs et al., 2013; Marin et al., 2013; Singels et al., 2014). For example, Cheeroo-Nayamuth et al. (2001) used the APSIM-sugarcane model (Keating et al., 1999) to simulate the sugarcane yield in Mauritius and found that larger reductions in sugarcane yield and sucrose production under increased temperature because of the lower water use efficiencies and high respiration demands irrespective of the change in rainfall. They concluded that irrigation was the best adaption option over others such as a change in cultivar or harvest date, but their assessment was based on simulations without considering the effects of CO_2 fertilisation on the physiology of the crop. However, Knox et al. (2010) used the DSSAT-Canegro model to explore the climate change impacts on sugarcane production in Swaziland and showed that the impacts of climate change can be offset by higher crop yields due to the direct effect of CO_2 fertilisation. Further, Marin et al. (2013) also using the DSSAT-Canegro model has shown that sugarcane yields are expected to increase by 24% by 2050 in southern Brazil based on earlier CMIP3 A2 and B2 CSIRO general circulation model (GCM) scenarios. More recent work by Singels et al. (2014) has also shown potential yield increases from 4 to 20% at representative sites in Australia, Brazil and South Africa from three GCMs to 2090. However, the possibility of negative net effects should not be overlooked (Everingham et al., 2015). Despite different scenarios the consideration of elevated [CO_2] in these sugarcane models points to likely increases in sugar yield as the climate changes with rising atmospheric CO_2 levels and warmer temperatures in the present major sugarcane production regions of the world. In addition, most of the previous studies have generated climatic inputs to the crop models by scaling historical observed climate using delta change method (Biggs et al., 2013; Knox et al., 2010; Marin et al., 2013; Webster et al., 2009) which merely considered the changes of climate means employing historical variance. The main limitation of such methodology is that it implicitly assumes that future temporal and spatial precipitation patterns are identical to that observed in the historical data.

The objectives of this study are to: (1) evaluate the performance of the APSIM-Sugarcane model using two-year's field experiment data in Guangxi, (2) investigate the future climate change impacts on sugarcane productivity in this region, and (3) identify the relationship between climate variables and sugarcane yields and examine strategies to cope with the impacts of climate change on sugarcane productivity in southern China.

2. Materials and methods

2.1. Study sites, climate and soil data

Guangxi is located in mountainous terrain in the far south of China. This region has a typical sub-tropical monsoon climate with long summer days and short winter days, high solar radiation and rainfall. Four sites, representing different climatic features within the region, were selected for this study (Fig. 1). Among these sites, Qinzhou is the hottest (annual average temperature of 22.7 °C) with highest rainfall (2149 mm). In contrast, Nanning has the lowest rainfall (1302 mm) with the second warmest temperature (22.5 °C). The remaining two

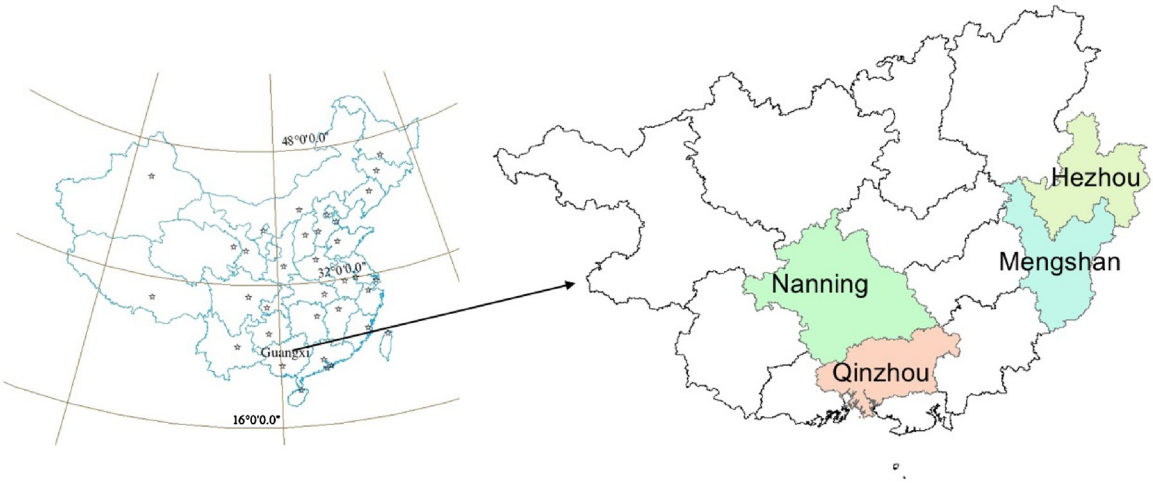

Fig. 1. The location of four study sites in Guangxi.

Table 1
Mean daily radiation, annual rainfall and annual temperature (1961–2010) at the four study sites.

Site	Latitude (°)	Longitude (°)	Elevation (m)	Radiation (MJ m^{-2})	Rainfall (mm)	Temperature (°C)
Hezhou	24.25	111.33	109	11.7	1549	20.7
Mengshan	24.13	110.53	146	11.6	1739	20.6
Nanning	22.63	108.22	122	12.7	1302	22.5
Qinzhou	21.97	108.65	5	13.1	2149	22.7

Table 2
The hydraulic properties of the soil used in simulations. (BD: bulk density; DUL: drained upper limit; SAT: saturated soil water content; LL15: lower limit 15 bar; AD: air dry).

Soil depth (cm)	BD (g cm^{-3})	LL15 (mm mm^{-1})	DUL (mm mm^{-1})	SAT (mm mm^{-1})	AD (mm mm^{-1})
0–10	1.51	0.11	0.32	0.36	0.08
10–20	1.52	0.11	0.31	0.35	0.08
20–30	1.54	0.12	0.30	0.34	0.09
30–45	1.63	0.13	0.28	0.31	0.10
45–60	1.59	0.15	0.28	0.32	0.10
60–90	1.55	0.15	0.28	0.32	0.14
100–130	1.55	0.15	0.27	0.31	0.14
130–160	1.64	0.16	0.26	0.30	0.15

Table 3
List of 28 GCMs under RCP4.5 and RCP8.5 future climate scenarios used in this study for statistical downscaling outputs of the four sites in Guangxi.

Model ID	Name of GCM	Abbr. of GCM	Institute ID	Country
01	BCC-CSM1.1	BC1	BCC	China
02	BCC-CSM1.1(m)	BC2	BCC	China
03	BNU-ESM	BNU	GCESS	China
04	CanESM2	CaE	CCCMA	Canada
05	CCSM4	CCS	NCAR	USA
06	CESM1(BGC)	CE1	NSF-DOE-NCAR	USA
07	CMCC-CM	CM2	CMCC	Europe
08	CMCC-CMS	CM3	CMCC	Europe
09	CSIRO-Mk3.6.0	CSI	CSIRO-QCCCE	Australia
10	EC-EARTH	ECE	EC-EARTH	Europe
11	FIO-ESM	FIO	FIO	China
12	GISS-E2-H-CC	GE2	NASA GISS	USA
13	GISS-E2-R	GE3	NASA GISS	USA
14	GFDL-CM3	GF2	NOAA GFDL	USA
15	GFDL-ESM2G	GF3	NOAA GFDL	USA
16	GFDL-ESM2M	GF4	NOAA GFDL	USA
17	HadGEM2-AO	Ha5	NIMR/KMA	Korea
18	INM-CM4	INC	INM	Russia
19	IPSL-CM5A-MR	IP2	IPSL	France
20	IPSL-CM5B-LR	IP3	IPSL	France
21	MIROC5	MI2	MIROC	Japan
22	MIROC-ESM	MI3	MIROC	Japan
23	MIROC-ESM-CHEM	MI4	MIROC	Japan
24	MPI-ESM-LR	MP1	MPI-M	Germany
25	MPI-ESM-MR	MP2	MPI-M	Germany
26	MRI-CGCM3	MR3	MRI	Japan
27	NorESM1-M	NE1	NCC	Norway
28	NorESM1-ME	NE2	NCC	Norway

sites were cooler with the average annual temperature around 20.7 °C and receive rainfall in the moderate-high range of 1500–1700 mm (Table 1). Daily values of maximum and minimum temperature, radiation, and rainfall for the four study sites from 1961 to 2016 were extracted from the China Meteorological Data Sharing Services System (CMDSSS) (http://adc.cma.gov.cn/home.do). These data were collected from automated weather stations at the sites. Soil variation in Guangxi is minimal and the dominant soil type at these study sites is a latosolic red soil (Dai et al., 2013). Therefore, this soil is representative of our study area. The hydraulic properties are shown in Table 2. Future climate data were derived from 28 Global Climate Models (GCMs) from the World Climate Research Program's (WCRP'S) Coupled Model Intercomparison Project phase 5 (CMIP5) dataset (Taylor et al., 2011). These projected climate data have been used in numerous climate impact studies (Anwar et al., 2015; Liu et al., 2017b; Wang et al., 2015; Yang et al., 2016). Table 3 provides some basic information for the 28 GCMs used in this study. Daily climate data for each location was generated from the monthly data of each GCM grids using the weather-generator based statistically downscaled model (NWAI-WG) developed by Liu and Zuo (2012) and inter-comparison of this downscaling model with other commonly used methods are available (Liu et al., 2017a). Briefly, this downscaling process consists of two steps: spatial downscaling and temporal downscaling. The first step was to interpolate the monthly projections of climate variables from GCM grid cells to monthly values for each of the sites of interest using an inverse distance-weighted (IDW) method. Bias correction was then applied to enable the resulting monthly site data to match with the observed data using a quantile mapping technique (Zhang, 2005, 2007), which plots the quantiles of observed climate data set against the quantiles of GCM projected climate data set in the same period. The second step was to disaggregate the monthly data to daily data through the modified WGEN stochastic weather generator (Richardson and Wright, 1984).

In this study, we assessed the response of sugarcane production to the changing climate in the three future periods of 2030s (2021–2040), 2060s (2051–2070) and 2090s (2081–2100) over the baseline period (1961–2010). The greenhouse gas CO_2 emissions of two different Representative Concentration Pathways (RCPs) (RCP4.5 and RCP8.5) were considered. These two scenarios were selected because they more closely represent current socio-economic conditions of radiative forcing and emissions (Wang et al., 2015), and have more data for monthly GCMs projections for statistical downscaling. Yearly atmospheric [CO_2] (ppm) for 1961–2100 are calculated for integrating into the APSIM-sugarcane simulation procedures, using the formulas in Eqs. (1) and (2) (Liu et al., 2014, 2017b).

$$[CO_2]_{RCP4.5} = 650.18 + \frac{7.5326 \times 10^{-5} y - 0.16276}{2.2299 \times 10^{-4} - 727.97 y^{-2}} - 1.8747 \times 10^{-4}(y - 2045)^3 \quad (1)$$

$$[CO_2]_{RCP8.5} = 1034.3 + \frac{267.78 - 1.6188 y}{4.0143 + 53.342 y^{-5.2882}} + 2.1746 \times 10^{-5}(y - 2020)^3 + 1.0065 \times 10^{-4}(y - 1911)^3 \quad (2)$$

where y is the calendar year with the values of y = 1961, 1962, …, 2100 for the year from 1961 to 2100.

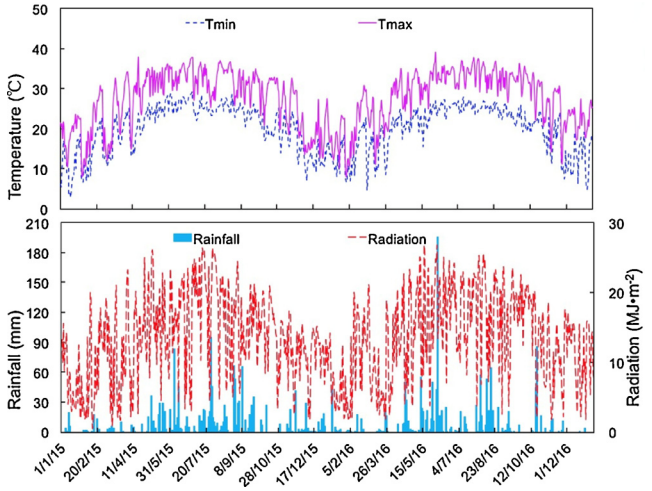

Fig. 2. Daily climate data during field experiments period in Nanning Agricultural Station. Tmax: maximum temperature (°C); Tmin: minimum temperature (°C).

2.2. Field experiments

The field experiments were conducted in 2015–2016 at the Agricultural Station at Nanning (22.63°N, 108.22°E). Daily climate data during the experiments are shown in Fig. 2. The experiments were designed with four planting dates (i.e., planting on 15 February 2015, 15 March 2015 and 5 April 2015 and 9 February 2016) as the main plots in a replicated blocked design (Table 4). There were three replicates butted together with no pathways, each 6 × 20 m plot comprised of 5 rows in 1.2 m row space with an additional edge row either side excluded from sampling. The first planting crop was harvested at 28 December 2015 and subsequently ratooned providing a fifth crop in the design. The cultivar planted was "Guitang32". The planting dates were randomised within each replicate. Prior to planting, NPK fertiliser was applied at the rate of 69 kg N ha^{-1}, 65 kg P ha^{-1}, and 30 kg K ha^{-1}. Additional fertilizer was applied on 100 days after planting at the rate of 69 kg N ha^{-1} and 30 kg K ha^{-1}. The same NPK fertiliser regime was applied to the ratooned crop, but the first fertiliser was applied two weeks after ratooning. Conventional land preparation and insect control measures were used for all treatments. All these crops were harvested periodically (20–80 days). A 1.5 m × 5 rows section of plot was harvested every time and stalk fresh mass was determined immediately. Above-ground biomass dry matter was determined after drying at 65 °C to constant weight. Sucrose content was determined using three randomly selected plants. Leaf area index (LAI) was determined using a LI-6400XT portable photosynthesis system. Sucrose and LAI determinations were mainly done in the last few samplings.

Notably, the sugarcane planted on 15 April 2015 experienced a long duration of large rainfall during the seeding stage, and suffered from the severe tropical storm "Kujira" (landfall on 21 June 2015) during the stalk elongating stage. Two plots of the experiment became waterlogged, and the condition lasted for three weeks. The sugarcane planted in these two blocks was severely damaged, and some died (approximately 20%). Thus, data obtained from these affected two plots were excluded.

Table 4
The planting/ratooning dates, harvest dates and plant type of sugarcane at Nanning station used for model calibration and validation.

Subsets	Planting/ratooning date	Harvest date	Plant type
Calibration	15/02/2015	27/12/2015	Plant
	28/12/2015	06/01/2017	Ratoon
Validation	15/03/2015	17/01/2016	Plant
	05/04/2015	22/02/2016	Plant
	09/02/2016	06/01/2017	Plant

2.3. Crop simulation

APSIM (Keating et al., 2003) is capable of analysing the effect of climate, soil and farm management on crop yield and has been widely validated and used around the world (Inman-Bamber and McGlinchey, 2003; Marin et al., 2013). APSIM-sugarcane is one of the crop models available in APSIM. It can simulate sugarcane crop growth, water use efficiency, N accumulation, biomass dry weight and fresh weight for plant and ratoon sugarcane in relation to climate, soil, genotypic factors and managements (Lisson et al., 2000). The main component of APSIM-sugarcane is crop dry weight accumulation and subsequent sugar yield (Keating et al., 1999), which is driven by the conversion of intercepted radiation to biomass, via radiation use efficiency (RUE). RUE is affected by the temperature, soil water and nitrogen (Marin et al., 2015).

The APSIM-sugarcane model can also simulate the effect of [CO_2] on plant growth. Marin et al. (2015) assessed the relative skill of the world's two most widely available and supported sugarcane models, i.e. APSIM-sugarcane and DSSAT/CANEGRO, in simulating sugarcane production under current and potential future climates in Brazil. The results illustrated that the two models had similar outputs under current climate, but APSIM-sugarcane exhibited a higher sensitivity to the increase of [CO_2] under potential future climate changes. However, this difference does not preclude its use in such an analysis. Generally, APSIM-sugarcane simulates the effect of atmospheric CO_2 on plant growth by regulating transpiration efficiency (TE) and RUE (Webster et al., 2009). They assumed that intrinsic TE would increase by 8% and RUE would increase by 1.43% for every 100 ppm increase in [CO_2] when simulating sugarcane yields for future climates in Australia, using the APSIM-Sugarcane model. In our study, we used the functions of Webster et al. (2009) to add the effect of elevated atmospheric [CO_2], on TE (g m^{-2} mm^{-1}) and RUE (g MJ^{-1}) such that:

$$TE(CO_2) = TE(350) \times \left(1 + \frac{[CO_2] - 350}{100} \times 0.08\right) \quad (3)$$

$$RUE(CO_2) = RUE(350) \times \left(1 + \frac{[CO_2] - 350}{100} \times 0.0143\right) \quad (4)$$

In this study, the APSIM-sugarcane version 7.7 was tested against the detailed field measurement data and used to quantify the potential impacts of future climate change on sugarcane productivity in Guangxi, South China. Simulations were performed for 1961–2100 in the four study sites. We used a typical crop cycle of one planting crop followed by three ratoon crops. The crop duration was 365 days for each planting crop and ratoon crop. Fertiliser applications in simulations were similar to field study site in Guangxi.

2.4. Model performance evaluation

The experimental data from planting date 15 February 2015 and ratooning crop on 28 December 2015 were used to calibrate model. RUEs for plant crops and ratoon crops observed in field experiments are 1.7–1.8 g MJ^{-1} and 1.6–1.7 g MJ^{-1}, respectively (Muchow et al., 1997). These values were obtained from the linear regression of accumulated biomass with the intercepted radiation and generally considered as a net value of RUE. Hence the default maximum RUE in APSIM-sugarcane is set to 1.8 g MJ^{-1}. In our initial simulations, this gave an underestimation of the observed values. Therefore, we used our experimental data and calibrated an RUE of 2.0 g MJ^{-1} in this environment. It is important to note that the same value was reported as the maximum RUE in Australia (Muchow et al., 1997) and close to the value of 2.06 g MJ^{-1} for crops grown in Hawaii (Meki et al., 2015). The key genetic parameters calibrated for sugarcane are listed in Table 5. For all the crops, parameters related to biomass and sugarcane growth

Table 5
Model parameters defining cultivars that were derived from experimental data of this study.

Parameter	Units	Description	Planting phrase	Ratoon phrase
cane_fraction	%	The fraction of daily produced above-ground biomass partitioned into cane	0.74	0.78
tt_emerg_to_begcane	°C day	Thermal time from the beginning of cane growth to flowering	1900	1600
RUE	g MJ^{-1}	Radiation-use efficiency	2	2

were derived using an iterative method with data from at least two seasons with contrasting climatic conditions used to achieve stable parameters. The calibrated model was then validated using the experimental data from the other three planting dates in 2015 and 2016 (Table 4) and additional 20 crops at six locations for fresh weight from Zu et al. (2018). The coefficient of determination (R^2), root mean square error (RMSE), and model efficiency (E) were used for evaluations of the model performance (Krause et al., 2005) as such;

$$R^2 = \left(\frac{\sum_{i=1}^{n} (O_i - \overline{O})(P_i - \overline{P})}{\sqrt{\sum_{i=1}^{n} (O_i - \overline{O})^2} \sqrt{\sum_{i=1}^{n} (P_i - \overline{P})^2}} \right)^2 \quad (5)$$

$$RMSE = \sqrt{\frac{\sum_{i=1}^{n} (O_i - P_i)^2}{n}} \quad (6)$$

$$E = 1 - \frac{\sum_{i=1}^{n} (O_i - P_i)^2}{\sum_{i=1}^{n} (O_i - \overline{O})^2} \quad (7)$$

where O_i and P_i denote observed and simulated values, $\overline{O}$ and $\overline{P}$ are their mean values, respectively. Generally, the smaller of RMSE, the smaller deviation between simulated and observed values. Additionally, the model simulates better than the mean of the observed data when $E \geq 0$, otherwise, if $E < 0$, then model prediction is worse than using the mean of the observations. The closer E is to 1, the more accurate the model is.

A descriptive statistical analysis was conducted by using least-squared multiple linear regression for estimating the contribution of various climate factors affecting sugarcane yields. The climate factors comprised changes in temperature, rainfall, radiation and [CO_2] from 28 GCMs' projections for three future periods (2030s, 2060s and 2090s).

3. Results

3.1. Model calibration and validation

The performance of the model was evaluated by comparing simulated and measured above-ground biomass dry matter (DM), stalk fresh mass (FM), leaf area index (LAI) and sucrose (S). In general, the model reasonably reproduced the dynamics and trends of these variables (Fig. 3). Specifically, the simulations of DM, FM and S closely followed the observations. However, some mismatches of LAI existed in the later stages.

When the model was validated, it was found that it provided good estimates of DM (Fig. 4a, RMSE = 7.21 t ha^{-1}) and S (Fig. 4c, RMSE = 0.88 t ha^{-1}). The model was able to explain 81% of the variation in DM, 82% in FM, 93% in S and 70% of the variation in LAI (Fig. 4). All the slopes of the regressions were also close to 1.0 (0.87–1.02), showing that the model is unbiased and together with low errors is considered to be satisfactory for the simulation of sugarcane growth in the study area. The E were greater than 0.0 with the values ranging from 0.68 to 0.92, suggesting the model can predicted relatively accurate values much more than using the mean of the observations. Notably, there were two observed FW measurements that were unexplained outliers (Fig. 4d), nevertheless the overall performance was considered acceptable for this study.

3.2. Projected future climate

The mean daily radiation for 1961–2010 at Hezhou, Mengshan, Nanning and Qinzhou were 11.7 MJ m^{-2}, 11.5 MJ m^{-2}, 12.6 MJ m^{-2} and 13.1 MJ m^{-2}, respectively (Table 1). Fig. 5a–d displayed the changes in daily radiation under the two scenarios. Our projections showed that compared with the baseline, the average radiation changed little for RCP4.5 by the 2030s at all four locations, while for RCP8.5, the average radiation decreased by approximately 1%. These decreases were in line with decreasing trends of observed radiation (Fig. S1a1–a8). However, the multi-model-mean radiation was overall expected to increase by up to approximately 6% during mid- and end-century period across four sites under two emission scenarios. At Nanning and Qinzhou, the annual mean daily radiation showed a similar increase in both two scenarios by the 2060s and 2090s, while at Hezhou and Mengshan RCP8.5 projected a higher radiation increase than RCP4.5. The largest shift in radiation was found at Mengshan especially under the high-emission RCP8.5 scenario, follow by Hezhou, where both had a multiple-GCMs ensemble mean of 6% increase. Despite the changing trends, both intra-annual (Table S1a and b) and inter-annual variability (Fig. 6a–d) of radiation had minor change in the future periods. Additionally, downscaled mean daily radiation and intra-annual variation for the baseline period were identical to historical observed values, confirming the reliability of the NWAI-WG downscaling results (Liu et al., 2017a).

The annual total rainfall for 1961–2010 at Hezhou, Mengshan, Nanning and Qinzhou were 1549 mm, 1739 mm, 1302 mm and 2149 mm respectively (Table 1). Projected annual total rainfall varied with GCMs, with some GCMs simulating increases in rainfall and some projecting decreases (Figs. 5e–h and S1b1–b8). Multi-model-mean values showed a slight increase in rainfall under RCP8.5 by 2030s across the four locations. Projected rainfall usually increased more under RCP4.5 during the near-future and mid-century period compared to values under RCP8.5 among study sites. For example, annual rainfall under RCP4.5 increased by 2.5% and 7.2% in 2030s and 2060s, respectively, at Nanning, while RCP8.5 led to a multi-model mean rainfall increase by 1.6% in 2030s and by 5.5% in 2060s. In contrast, by the 2090s, RCP8.5 projected a slightly more increased rainfall than RCP4.5 at Nanning and Qinzhou. The coefficients of variation (CVs) also showed small increases, pointing to higher variability of inter-annual rainfall into the future (Fig. 6e–h). However, changes in the intra-annual variability were small relative to baseline period (Table S1c, d).

The annual mean daily temperature for 1961–2010 at Hezhou, Mengshan, Nanning and Qinzhou were 20.7 °C, 20.6 °C, 22.5 °C and 22.7 °C respectively (Table 1). Fig. 5i–j shows changes in temperature projected by 28 GCMs under RCP4.5 and RCP8.5, relative to the baseline period at the four locations. Overall, RCP8.5 projected a more increase in temperature than RCP4.5. Our results indicated that annual mean temperature increased progressively in 2030s, 2060s and 2090s for both RCPs. For example, the mean increases in temperature at Mengshan were 0.9 °C for 2030s, 1.7 °C for 2060s and 2.1 °C for 2090s under RCP4.5 (Fig. 5i). Similar changes could be found at the other sites. The temporal variations of annual mean temperature are shown in Fig. S1c1–c8. Similar increasing trends were found in all four sites. In addition, both intra-annual (Table S1e, f) and inter-annual (Fig. 6i–l) variability of annual mean temperature had small decreases.

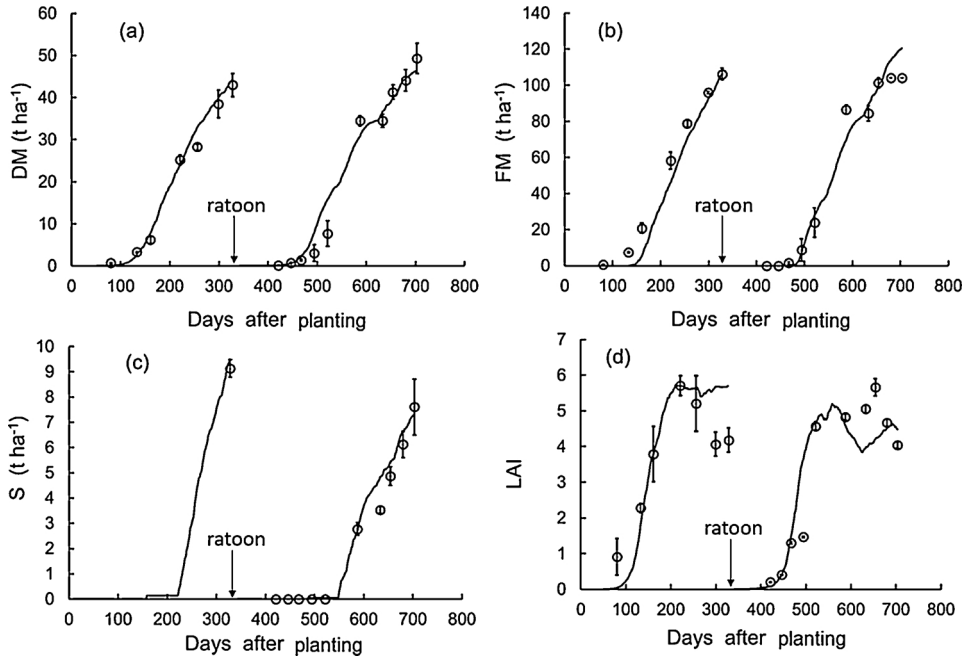

Fig. 3. Comparison of simulated (line) and observed (circles) of sugarcane (a) above-ground dry matte (DM), (b) stalk fresh mass (FM), (c) sucrose (S) and (d) leaf area index (LAI) for the calibration subset (Table 4).

3.3. Projected phenology changes and sugarcane yields

Changes in days from planting/ratoon to cane appearance (DTCA) are shown in Fig. 7a–d. Obvious decreases were projected for all four sites and all three future periods. Overall, DTCA had greater decreases under RCP8.5, compared to RCP4.5. The greatest shortening of DTCA was projected at Mengshan during 2090s under RCP8.5, reaching 20 days. It was clear that the increases of temperature (Figs. 5 and S1) were the major driver in resulting in the shortening of DTCA.

The simulated annual mean DM during 1961–2010 was 19.4, 23.2, 28.4 and 37.4 t ha^{-1} at Hezhou, Mengshan, Nanning and Qinzhou, respectively. This large range in DM across four locations was caused by the limitation of the dominated climatic variables of radiation, temperature and water supply. Fig. 7a–d shows DM changes over three future time periods as simulated using the APSIM-sugarcane model based on 28 GCMs under RCP4.5 and RCP8.5 scenarios. Overall, future mean DM were projected to increase by 5.6 and 6.4 and 6.6 t ha^{-1} for RCP4.5 and 5.1, 6.1 and 5.8 t ha^{-1} for RCP8.5, respectively for 2030s, 2060s and 2090s. RCP8.5 had less promotion compared to RCP4.5 on DM. There were small differences in simulated DM change among the four locations. The largest increase in DM change was found at Qinzhou, especially under the RCP4.5 scenario. The average DM simulated from the different GCM projected climate varied most (5th–95th percentages) for the 2090 period, followed by 2060 period,

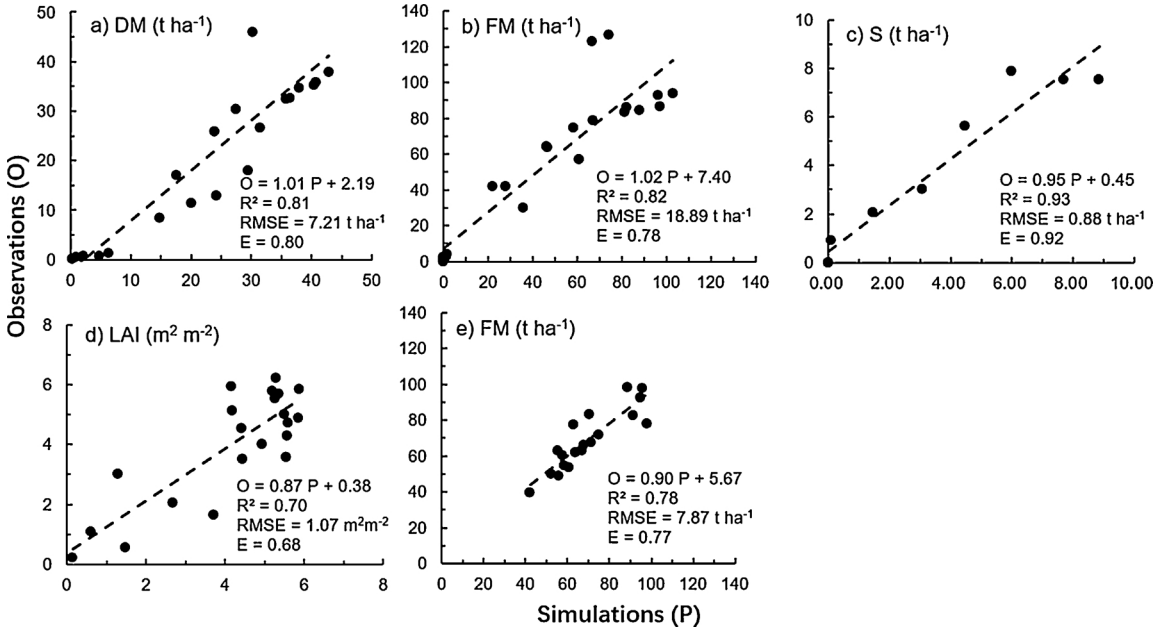
a) DM (t ha-1)
O = 1.01 P + 2.19
R² = 0.81
RMSE = 7.21 t ha-1
E = 0.80
b) FM (t ha-1)
O = 1.02 P + 7.40
R² = 0.82
RMSE = 18.89 t ha-1
E = 0.78
c) S (t ha-1)
O = 0.95 P + 0.45
R² = 0.93
RMSE = 0.88 t ha-1
E = 0.92
d) LAI (m2 m-2)
O = 0.87 P + 0.38
R² = 0.70
RMSE = 1.07 m2m-2
E = 0.68
e) FM (t ha-1)
O = 0.90 P + 5.67
R² = 0.78
RMSE = 7.87 t ha-1
E = 0.77
Observations (O)
Simulations (P)

Fig. 4. Comparison of simulated (P) and observed (O) values of sugarcane (a) above-ground dry matter (DM), (b) stalk fresh mass (FM), (c) sucrose (S) and (d) leaf area index (LAI) for the validation subset (Table 4). Additional validation data from Zu et al. (2018) are shown in (e).

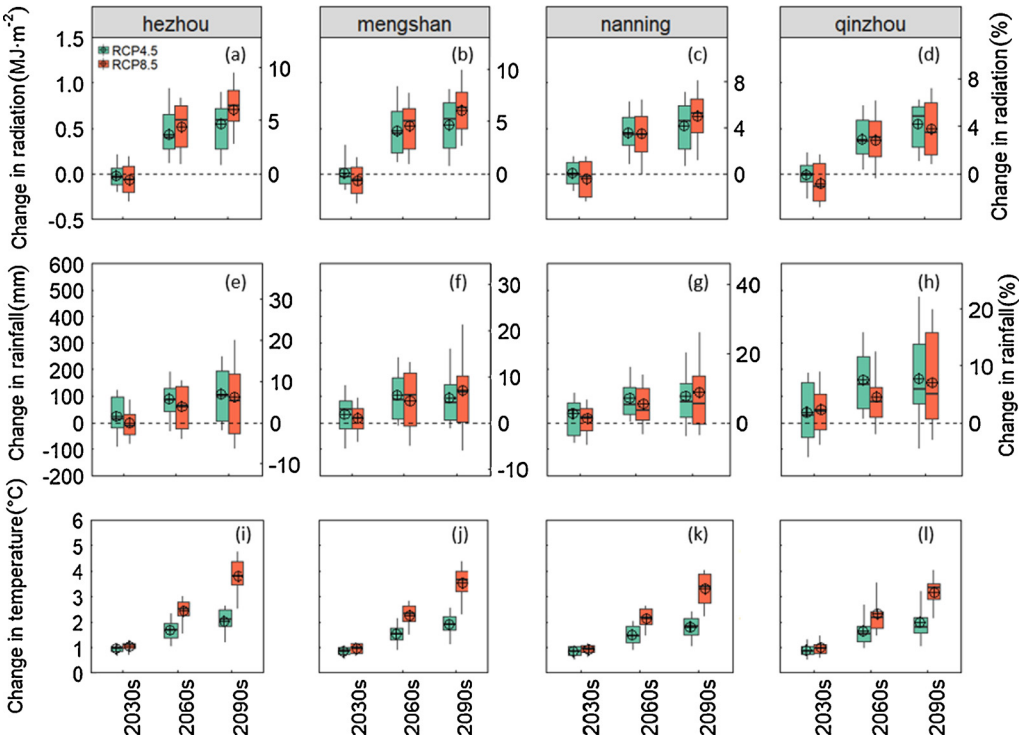

Fig. 5. Projected changes in daily mean radiation, annual rainfall and annual average temperature under RCP4.5 and RCP8.5 at four study sites. Data were presented as change between 1961 and 2010 and three future time periods (2021–2040, 2051–2070 and 2081–2100) based on the 28 downscaled GCMs. The percentage data are shown on the right-hand y-axis and the left-hand y-axis shows the change in absolute values. Each box consists of 28 values. Box boundaries indicate the 25th and 75th percentiles across GCMs, whiskers below and above the box indicate the 10th and 90th percentiles. The black lines and crosshairs within each box indicate the multi-model median and mean respectively.

and Nanning was the most variable location. Even though there were large variations in DM change across the four locations, the overall change in DM values of 28 GCMs was increasing in all future climates relative to baseline under two RCPs (Fig. S2a1–a8). Inter-annual variability of DM slightly increased at Nanning, but minor decreases in the other 3 sites were evident in the future periods (Fig. 8e–h).

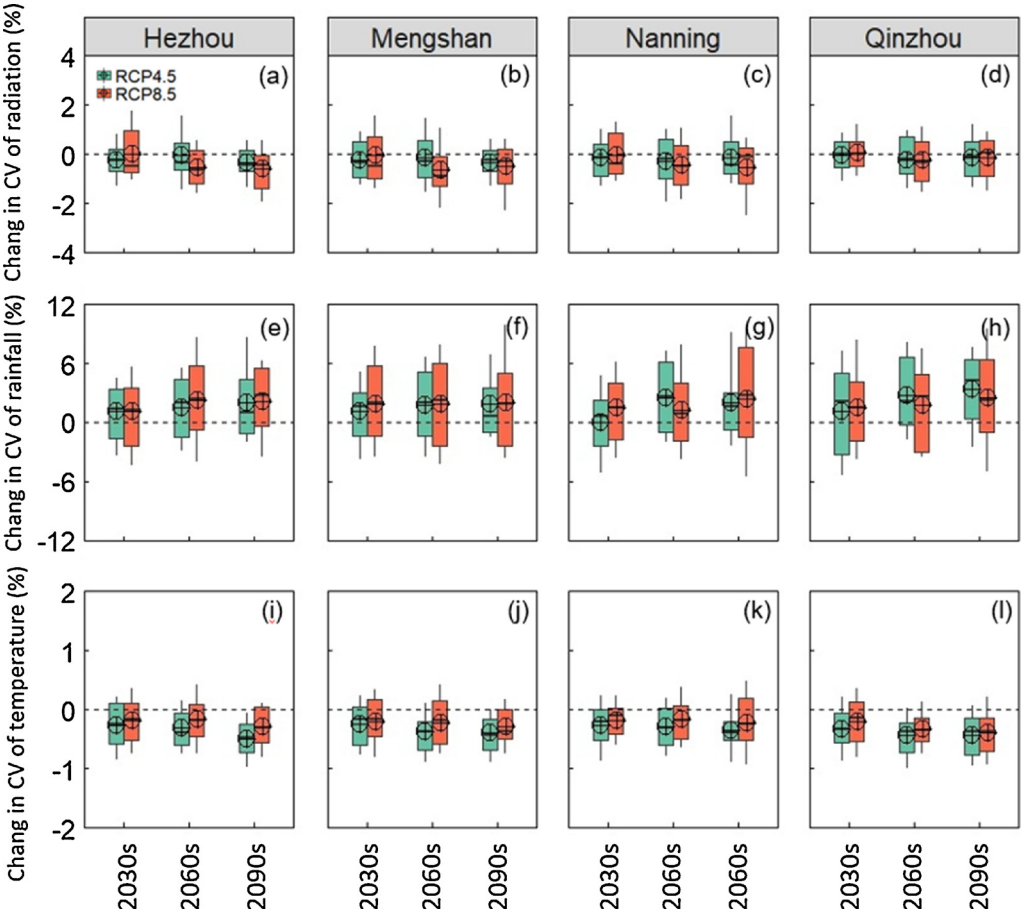

Fig. 6. Projected changes in the coefficient of variation (CV) of mean annual total rainfall, mean annual temperature and mean annual daily solar radiation under RCP4.5 and RCP8.5 at four stations. Data were presented as change between 1961 and 2010 and three future time periods (2021–2040, 2051–2070 and 2081–2090) based on the 28 downscaled GCMs. Each box consists of 28 values. Box boundaries indicate the 25th and 75th percentiles across GCMs, whiskers below and above the box indicate the 10th and 90th percentiles. The black lines and crosshairs within each box indicate the multi-model median and mean respectively.

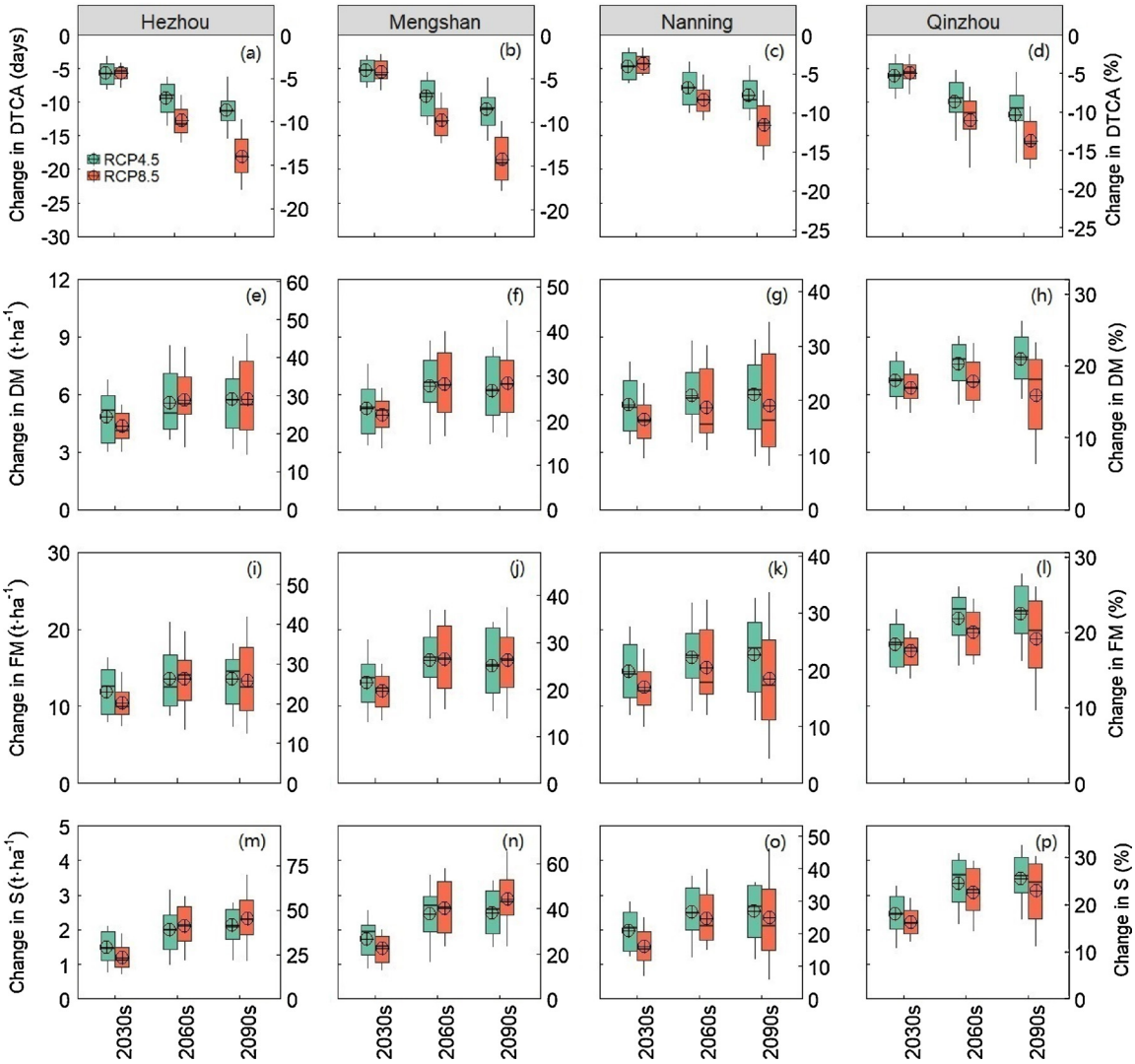

Fig. 7. Simulated changes in days to cane appearance (DTCA), sugarcane biomass dry matter (DM), stalk fresh mass (FM) and sucrose dry matter (S) under RCP4.5 and RCP8.5 at four study sites. Data were presented as change between 1961 and 2010 and three future time periods (2021–2040, 2051–2070 and 2081–2100) based on the 28 downscaled GCMs. The percentage data are shown on the right-hand y-axis and the left-hand y-axis show the change in absolute values. Box boundaries indicate the 25th and 75th percentiles across GCMs, whiskers below and above the box indicate the 10th and 90th percentiles. The black lines and crosshairs within each box indicate the multi-model median and mean respectively.

Fig. 7e–h shows the changes in simulated FM between the baseline (1961–2010) and the future climate (2030s, 2060s and 2090s) for each location. The changes of FM were generally identical to DM across all locations. The FM change values increased more under RCP4.5 than under RCP8.5 at all locations. The largest increase in FM change was also found at Qinzhou under RCP4.5. Temporal variation of FM was shown in Fig. S2b1–b8. FM yields had large fluctuations across the planted and ratoon crops, but overall upward trends were detected in almost all the four sites under the two RCP scenarios. Inter-annual variability of FM had small changes in the future periods (Fig. 8i–l).

Compared with the baseline (1961–2010), the overall change in S was positive in all future climates across all locations (Fig. 7i–l). The simulated annual S in the baseline period were around 5.1, 6.5, 9.4 and 13.7 t ha^{-1} at Hezhou, Mengshan, Nanning and Qinzhou respectively (Fig. S2c1–c8). The largest change in S consistently occurred at Qinzhou, with an average change of 2.4 and 2.2 t ha^{-1} for RCP4.5 and RCP8.5 in 2030s, 3.3 and 3.1 kg ha^{-1} in 2060s, and 3.7 and 3.0 t ha^{-1} for in 2090s, respectively. However, the largest percentage change in S occurred at Hezhou, with mean values of percentage change were 28.1% and 39.4% for RCP4.5 and RCP8.5 in 2030s, 44.2% and 23.5% in 2060s, and 41.1% and 45.5% for in 2090s, respectively. This was likely to be due to Hezhou having relatively a low rainfall and mean temperature during the baseline period (Table 1), but the increases in rainfall and mean temperature across the four sites were similar for the future periods (Fig. 5). Similar to DM, inter-annual variability of S had a slightly increased variability at Nanning, but decreased at the other three sites (Fig. 8m–p).

3.4. Sugarcane yield relationship with future climate

Prior to identifying the contribution of the changes in climate variables to crop yield change, we calculated the variance inflation factor (VIF) to detect collinearity of input variables. The results are shown in Table S2. Generally, a VIF value less than 10 is an acceptable threshold in climate related studies (Doetterl et al., 2015). All the four predictors (change in radiation, temperature, rainfall and [CO_2]) were satisfactory and had VIF values less than 10 at the four sites. Table 6 shows the results of regressions. Across all locations, increases in sugarcane yields were strongly correlated (P = .001) with each Celsius degree increase in future temperature and per mm increase in future rainfall. For example, the DM, FM and S increased 14.2, 36.1 and 6.1 kg ha^{-1} mm^{-1} in response to rainfall, respectively at Nanning,

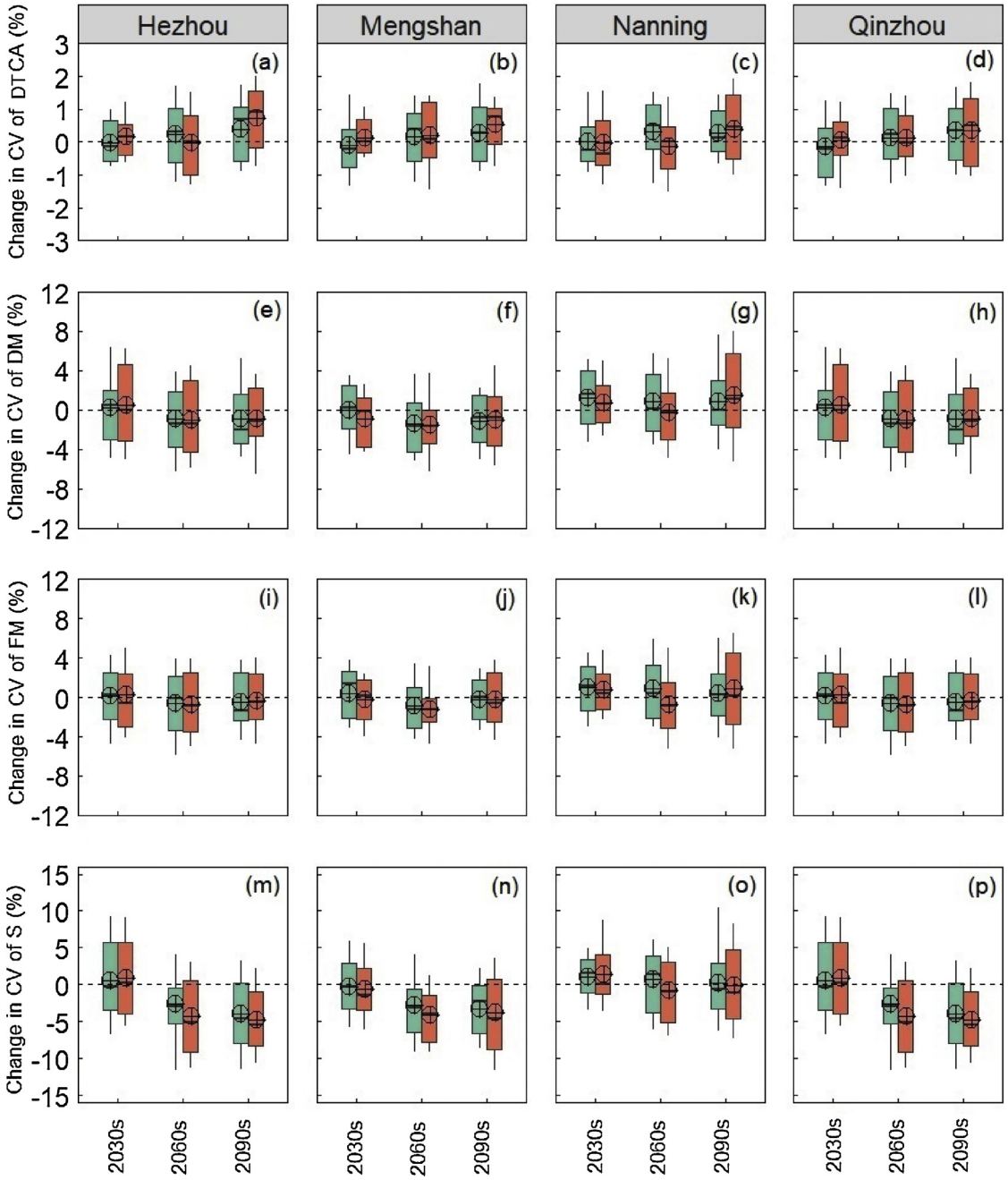

Fig. 8. Simulated changes in the coefficient of variation (CV) of days to cane appearance (DTCA), sugarcane biomass dry matter (DM), stalk fresh mass (FM) and sucrose dry matter (S) based on 28 GCMs at four locations under RCP4.5 and RCP8.5 in 2030s, 2060s and 2090s relative to baseline period (1961–2010). Box boundaries indicate the 25th and 75th percentiles across GCMs, whiskers below and above the box indicate the 10th and 90th percentiles. The black lines and crosshairs within each box indicate the multi-model median and mean respectively.

which had the largest increase in yield response to rainfall in the four locations. This was likely to be due to the similar changes in rainfall in the future and the lowest mean annual total rainfall during the baseline at Nanning (Fig. 5 and Table 1). Generally, CO_2 had little effects on sugarcane yields, but it had significant ($P < 0.05$) effects on DM, FM and S at Qinzhou. The results were similar to Cheeroo-Nayamuth et al. (2001), which showed that high [CO_2] in raising sugarcane yields is mainly due to water supply. While for radiation, it had significant effects on S but little effects on DM and FM. Generally, the four climate factors could explain more than 70% of the sugarcane yield changes likely in the future.

4. Discussion

The application of any well-known crop model to a new environment usually requires re-calibration of some variables, particularly if the experimental sites are much different from those where the models has been previously developed or shown to be satisfactory. We tested the published uncalibrated APSIM-sugarcane model at our study sites and recalibration of three parameters was necessary. Our parameterisation included raising the maximum RUE from 1.8 to 2.0 g MJ^{-1} and the subsequent validation showed that there was a good general agreement between simulated and observed values. For example, the R^2 and RMSE values obtained between the simulated and measured DM were 0.81 and 7.21 t ha^{-1}, respectively. Similar results were also

Table 6
The coefficients of the regression analysis (*a, b, c, d*) of the impact rates of climate change on sugarcane yields at Hezhou, Mengshan, Nanning and Qinzhou, respectively. The change in yield (ΔY, where Y = DM, FW or S in kg ha^{-1}) as functions of the change in annual total rainfall (ΔP, kg ha^{-1} mm^{-1}), daily mean solar radiation (ΔR, kg ha^{-1} (MJ m^{-2}) $^{-1}$), daily mean temperature (ΔT, kg ha^{-1} $°C^{-1}$), and CO_2 concentration (ΔCO_2, kg ha^{-1} ppm^{-1}) are shown in the figures.

Site	*a*	*b*	*c*	*d*	R^2
$\Delta DM = a\Delta R + b\Delta P + c\Delta T + d\Delta CO_2$					
Hezhou	−0.99	9.12***	2123***	−0.01	0.77
Mengshan	1.48	7.79***	2210***	−0.00	0.78
Nanning	−3.24	14.15***	3092***	−7.52*	0.71
Qinzhou	0.05	6.69***	1379***	7.40*	0.70
$\Delta FM = a\Delta R + b\Delta P + c\Delta T + d\Delta CO_2$					
Hezhou	−0.32	25.72***	4593***	−1.37	0.75
Mengshan	6.47	20.45***	4881***	2.79	0.78
Nanning	−6.29	36.14**	8417***	−19.06	0.74
Qinzhou	1.79	16.59***	4594***	18.28*	0.74
$\Delta S = a\Delta R + b\Delta P + c\Delta T + d\Delta CO_2$					
Hezhou	1.55**	3.75***	618***	−0.26	0.81
Mengshan	2.86***	3.13***	655***	0.43	0.84
Nanning	0.97	6.06***	1093***	−2.77	0.76
Qinzhou	3.05**	2.65***	637***	2.35*	0.79

*, ** and *** indicate the significant at the level of $P < 0.05$, $P < 0.01$ and $P < 0.001$, respectively.

achieved in the sugarcane study conducted by Ojeda et al. (2017). There was also sufficiently good agreement between simulated and observed FM and LAI as well as S with mean errors typical of other sugarcane models (Liu and Bull, 2001; O'Leary, 2000). Given the relatively low errors the model captured the main biophysical variables (e.g. LAI, radiation extinction and radiation use efficiency) to ascribe environmental causation in determining sugar yields.

Our results showed that all GCMs agree on a future growing season temperature increase. Future climate projections from the multi-model values based on the 28 GCMs showed an averaged warming of 0.9 °C for RCP4.5 and 1.0 °C for RCP8.5 across the four locations by 2030s compared to the baseline period 1961–2010. This finding was consistent with results of Zhang et al. (2008), that projected an increase of 1.1 °C by 2030 (mean projection) for inland China under a medium emission scenario. However, not all GCMs within an ensemble accorded with the sign of rainfall change (Fig. 5e–h). There were large differences in magnitude and sign among GCMs. Similar patterns could also be found in radiation change. Despite some dissimilarity on the direction of change, the multi-model ensemble mean values showed the increase in growing season rainfall of 2.0% under RCP4.5 and 1.1% under RCP8.5 across locations. The magnitude of this increase became larger in the far-future change period than that for the near-future period. These changes were also in line with the findings of Ding et al. (2006), which concluded that the average annual rainfall in China will increase by 2%–3% and 5%–7% in 2020 and 2050, respectively.

Previous studies have used outputs from fewer multiple climate models with crop simulation models to investigate the impact of climate change on sugarcane. Most of these have generated inputs to the crop model by scaling historical climate observations with simulated climate changes (Ludwig and Asseng, 2006; Wang et al., 2009). However, the scaling methods or climate change factors neglected the effects of inter-annual climate variability (Liu et al., 2017a). In contrast, statistical downscaling used in our study can capture the variation of annual temperature and rainfall as well as radiation (Anwar et al., 2015; Liu and Zuo, 2012), which more realistically represent future climate conditions. In the present study, the statistical downscaling GCM daily climate data were used to drive the calibrated APSIM-sugarcane model to evaluate the effects of future climate change on sugarcane productivity in southern China. Our simulations projected that multi-model mean sugarcane FM increased by 20.6% under RCP4.5 and 18.5% under RCP8.5 compared with baseline climate across the four locations by 2030s. In addition to the increase of FM, future climate projections would also increase the DM and S. These increases can be attributed to increased growing season temperature and rainfall based on projections of the GCMs (Table 3). Temperature-induced decreases in DTCA (Fig. 7) also contributed to yield increases, because there is more time to grow and store sugar if the cane appears earlier. Our simulated results were consistent with Marin et al. (2013), that showed FM would increase 24% for rainfed sugarcane under two GCM projections of increased temperature, elevated [CO_2] and increased rainfall in Brazil. This increase in sugar yield is important for this region of Asia and likely in other sugar producing regions of the world.

Physiologically, sugarcane is a C4 plant and has higher photosynthetic rates and is more efficient than C3 plants at the same [CO_2]. It is reported that RUE in sugarcane can be up to 2.0 g MJ^{-1} of intercepted photosynthetically active radiation (Muchow et al., 1997) in unstressed water and nutrient conditions without very high temperatures. In theory, increases in [CO_2], high mean temperature and solar radiation can improve photosynthesis and increase yields (Hasegawa et al., 2013). Therefore, together with increases in [CO_2], temperature and solar radiation changes are likely to have a significant effect on sugarcane production. De Souza et al. (2008) reported that sugarcane under elevated [CO_2] showed an increase in about 30% in photosynthesis and accumulated 40% more biomass in comparison with the plants grown at ambient [CO_2], which are associated with higher water-use efficiency and lower stomatal conductance and transpiration rate. However, in our study we did not observe more sugarcane yield increases under RCP8.5 compared to RCP4.5 especially in the 2090s when large differences in [CO_2] occurred between the two RCPs, even though we included the effects of [CO_2] through TE and RUE. In addition, the contribution of elevated [CO_2] to sugarcane DM and FM increase was not significant at Mengshan, Hezhou or Nanning (Table 3). This is not surprising as other studies have also reported that under well-irrigated conditions, elevated [CO_2] might not cause any substantial increase in yield for sugarcane with its primary effect on reducing transpiration (Inman-Bamber et al., 2016; Stokes et al., 2016).

Inevitably, there were some uncertainties and limitations in the approach used in our study that linked climate scenarios and crop modelling. Crop models are powerful and effective tools in predicting the effects of future climate change on crop productivity because they allow objective analyses that are not possible by traditional field or controlled environment experimentation. However, they have presented some simplified processes of plant growth and soil processes. Although a number of simplifications are necessary for efficient simulation, they limit the accuracy of the simulated crop response to environmental conditions. For example, the model does not account for the effect of extreme weather events (e.g. rainstorms or typhoons) on lodging events and soil conditions (e.g. waterlogging, salinity, acidity and/or fertility). The selection of soils for the simulation and the cultivar calibration used were also sources of uncertainty. The model response to CO_2 also needs to be validated with more field experiments because of its sensitivity to stomatal conductance and transpiration, compared to other crops like wheat. Moreover, the limitations of GCMs mean that the climate data used to drive the model simulations in this study may not accurately project real future climate conditions due to uncertainties of actual greenhouse gas emissions. Although we applied a sophisticated statistical downscaling method to generate daily climate data as inputs of crop model, the statistical downscaling method also has limitations, such as changes in the frequency of extreme events (e.g. droughts or heatwaves), and if these are large could change the results observed here.

Our results show that in some low latitude locations (e.g. Qinzhou) where sugarcane benefits from a favorable climate (sufficient light, temperature and rainfall), therefore, increasing atmospheric [CO_2] significantly contributes to yield increase (Table 6). By contrast, the

baseline sugarcane yield in high latitude locations (e.g. Hezhou) is much lower than that in the low latitude locations. However, their response to future climate change is large due to their low present yields (Fig. 7). This means that a small magnitude of climate change will have a substantial contribution to yields in high latitude areas. Zu et al. (2018) has shown that the spatial distribution of potential sugarcane yields increased with decreasing latitude because sugarcane yields were mainly limited by solar radiation and temperature in that part of China. Therefore, there is a great potential for high latitude locations to achieve more yield if suitable management options or new cultivars are implemented, especially when future climate change is beneficial. Our study implies that it is very important to breed new sugarcane cultivars that are more tolerant to lower radiation to have better radiation utilisation in high latitude areas of China. It is also critical to introduce high-yield management practices, e.g., weed and pest control, integrated mechanisation, and change agricultural production policies, e.g., increase financial subsidies, for these regions. While not specifically addressed in this study, there are clear advances to be made with new technology in managing agronomic resources as well as breeding new cultivars of sugarcane that are also more resistant to lodging and extreme weather events. Despite uncertainties in future climate change from 28 different GCMs and two different scenarios for future greenhouse gas forcing of the climate system (RCP4.5 and RCP8.5), the results from this study could be useful for policymakers to develop relevant strategies for increasing sugarcane productivity in southern China. It is anticipated that other parts of Asia and tropical and subtropical regions similar to our study area will also benefit from the likely changes in future climate.

5. Conclusion

The APSIM-Sugarcane model has been well validated in southern China. Statistical downscaling climate data projected a small increase in rainfall and radiation with large variations among the 28 GCMs. However, all GCMs projected a progressively increased temperature in 2030s, 2060s and 2090s for both RCP4.5 and 8.5. The calibrated APSIM-Sugarcane model analysing downscaling climate data based on 28 GCMs under two RCPs, showed an overall positive impact of climate change on sugarcane yield across four locations in southern China. This was due to increased temperature, radiation and rainfall together with elevated [CO_2]. However, the magnitude of increased yields depended on locations and GCMs. Generally, high latitude locations presented a larger increase in yields than that in the low latitude locations due to the limitation of radiation and temperature. The large gap in yield between high-latitude and low-latitude regions indicates a huge potential to increase sugarcane yield in high-latitude areas through breeding more tolerant to lower radiation to fully use the benefits of climate change. It is also important to develop cultivars that are resistant to lodging to adapt extreme weather events (e.g. typhoons). In addition, market and policy incentives from local government may be required to assist the sugar industry to adapt to the changing climate in southern China. Our results are pivotal for providing a sound basis for policymakers to make strategies to achieve high sugarcane yields in China.

Acknowledgements

The senior author acknowledges that this work was supported by Cultivation Base of Guangxi Key Laboratory for Agro-Environment and Agro-Product Safety (2016, 133), and the Study Abroad Program for Excellent Ph.D. Students of Guangxi Zhuang Autonomous Region, China. New South Wales Department of Primary Industries provided office facilities for the senior author's visiting study. We acknowledge the World Climate Research Programme's Working Group on Coupled Modelling, which is responsible for CMIP, and we thank the climate modelling groups for producing and making available their model output. For CMIP the US Department of Energy's Program for Climate Model Diagnosis and Intercomparison provides coordinating support and led development of software infrastructure in partnership with the Global Organisation for Earth System Science Portals. Thanks to Dr Ian Macadam of Climate Research Centre and ARC Centre of Excellence for Climate System Science, University of New South Wales, Sydney for downloading GCM data.

Appendix A. Supplementary data

Supplementary data associated with this article can be found, in the online version, at https://doi.org/10.1016/j.eja.2018.03.007.

References

Anwar, M.R., Liu, D.L., Farquharson, R., Macadam, I., Abadi, A., Finlayson, J., Wang, B., Ramilan, T., 2015. Climate change impacts on phenology and yields of five broadacre crops at four climatologically distinct locations in Australia. Agric. Syst. 132, 133–144.

Biggs, J.S., Thorburn, P.J., Crimp, S., Masters, B., Attard, S.J., 2013. Interactions between climate change and sugarcane management systems for improving water quality leaving farms in the Mackay Whitsunday region, Australia. Agric. Ecosyst. Environ. 180, 79–89.

Bull, T., Glasziou, K., 1979. Sugarcane, chapter 4. In: Lovett, J.V., Lazenby, A. (Eds.), Australian Field Crops Volume 2: Tropical Cereals, Oilseeds, Grain Legumes and Other Crops. Angus and Robertson Publishers, pp. 95–113.

Cheeroo-Nayamuth, F.B., Nayamuth, R.A.H., Hogarth, D.M., 2001. Climate change and sucrose production in Mauritius. In: Proceedings of the XXIV Congress, Brisbane, Australia. International Society of Sugar Cane Technologists 24. pp. 107–112.

Dai, Y., Shangguan, W., Duan, Q., Liu, B., Fu, S., Niu, G., 2013. Development of a China dataset of soil hydraulic parameters using pedotransfer functions for land surface modeling. J. Hydrometeorol. 14, 869–887.

De Souza, A.P., Gaspar, M., Da Silva, E.A., Ulian, E.C., Waclawovsky, A.J., Dos Santos, R.V., Teixeira, M.M., Souza, G.M., Buckeridge, M.S., 2008. Elevated CO2 increases photosynthesis, biomass and productivity, and modifies gene expression in sugarcane. Plant Cell Environ. 31, 1116–1127.

Ding, Y., Ren, G., Shi, G., Peng, G., Zheng, X., Zhai, P., Zhang, D., Zhao, Z., Wang, S., Yong, L., 2006. National Assessment Report of Climate Change (I): climate change in China and its future trend. Adv. Clim. Change Res. 03, 1–5.

Doetterl, S., Stevens, A., Six, J., Merckx, R., Oost, K.V., Pinto, M.C., Casanovakatny, A., Muñoz, C., Boudin, M., Venegas, E.Z., 2015. Soil carbon storage controlled by interactions between geochemistry and climate. Nat. Geosci. 8.

Everingham, Y., Inman-Bamber, G., Sexton, J., Stokes, C., 2015. A dual ensemble agro-climate modelling procedure to assess climate change impacts on sugarcane production in Australia. Agric. Sci. 6, 870–888.

Hasegawa, T., Sakai, H., Tokida, T., Nakamura, H., Zhu, C.W., Usui, Y., Yoshimoto, M., Fukuoka, M., Wakatsuki, H., Katayanagi, N., Matsunami, T., Kaneta, Y., Sato, T., Takakai, F., Sameshima, R., Okada, M., Mae, T., Makino, A., 2013. Rice cultivar responses to elevated CO2 at two free-air CO2 enrichment (FACE) sites in Japan. Funct. Plant Biol. 40, 148–159.

Huang, C., Zhang, W., Jian, S., 2006. Comparison of important characters and productive status between sugarbeet and sugarcane in China. Sugar Crops China 2, 41–44.

Inman-Bamber, N., McGlinchey, M., 2003. Crop coefficients and water-use estimates for sugarcane based on long-term Bowen ratio energy balance measurements. Field Crops Res. 83, 125–138.

Inman-Bamber, N., Jackson, P., Stokes, C., Verrall, S., Lakshmanan, P., Basnayake, J., 2016. Sugarcane for water-limited environments: enhanced capability of the APSIM sugarcane model for assessing traits for transpiration efficiency and root water supply. Field Crops Res. 196, 112–123.

Keating, B.A., Robertson, M.J., Muchow, R.C., Huth, N.I., 1999. Modelling sugarcane production systems I. Development and performance of the sugarcane module. Field Crops Res. 61, 253–271.

Keating, B.A., Carberry, P.S., Hammer, G.L., Probert, M.E., Robertson, M.J., Holzworth, D., Huth, N.I., Hargreaves, J.N., Meinke, H., Hochman, Z., 2003. An overview of APSIM, a model designed for farming systems simulation. Eur. J. Agron. 18, 267–288.

Knox, J.W., Díaz, J.A.R., Nixon, D.J., Mkhwanazi, M., 2010. A preliminary assessment of climate change impacts on sugarcane in Swaziland. Agric. Syst. 103, 63–72.

Krause, P., Boyle, D., Bäse, F., 2005. Comparison of different efficiency criteria for hydrological model assessment. Adv. Geosci. 5, 89–97.

Li, Y.R., Yang, L.T., 2015. Sugarcane agriculture and sugar industry in China. Sugar Tech 17, 1–8.

Li, Y.R., Wu, J.M., Li, X., Zhang, R.H., Liu, X.H., Yang, L.T., 2015. Damage in sugarcane production caused by long duration of chilling and frost in Guangxi, China. Int. J. Agric. Innov. Res. 3, 1139–1144.

Lisson, S.N., Robertson, M.J., Keating, B.A., Muchow, R.C., 2000. Modelling sugarcane production systems – II: analysis of system performance and methodology issues. Field Crops Res. 68, 31–48.

Liu, D.L., Bull, T.A., 2001. Simulation of biomass and sugar accumulation in sugarcane using a process-based model. Ecol. Model. 144, 181–211.

Liu, D.L., Zuo, H., 2012. Statistical downscaling of daily climate variables for climate change impact assessment over New South Wales, Australia. Clim. Change 115,

629–666.
Liu, D.L., Anwar, M.R., O'Leary, G., Conyers, M.K., 2014. Managing wheat stubble as an effective approach to sequester soil carbon in a semi-arid environment: spatial modelling. Geoderma 214, 50–61.
Liu, D.L., O'Leary, G.J., Christy, B., Macadam, I., Wang, B., Anwar, M.R., Weeks, A., 2017a. Effects of different climate downscaling methods on the assessment of climate change impacts on wheat cropping systems. Clim. Change 1–15.
Liu, D.L., Zeleke, K.T., Wang, B., Macadam, I., Scott, F., Martin, R.J., 2017b. Crop residue incorporation can mitigate negative climate change impacts on crop yield and improve water use efficiency in a semiarid environment. Eur. J. Agron. 85, 51–68.
Ludwig, F., Asseng, S., 2006. Climate change impacts on wheat production in a Mediterranean environment in Western Australia. Agric. Syst. 90, 159–179.
Marin, F.R., Jones, J.W., Singels, A., Royce, F., Assad, E.D., Pellegrino, G.Q., Justino, F., 2013. Climate change impacts on sugarcane attainable yield in southern Brazil. Clim. Change 117, 227–239.
Marin, F.R., Thorburn, P.J., Nassif, D.S., Costa, L.G., 2015. Sugarcane model intercomparison: structural differences and uncertainties under current and potential future climates. Environ. Model. Softw. 72, 372–386.
Meki, M.N., Kiniry, J.R., Youkhana, A.H., Crow, S.E., Ogoshi, R.M., Nakahata, M.H., Tirado-Corbalá, R., Anderson, R.G., Osorio, J., Jeong, J., 2015. Two-year growth cycle sugarcane crop parameter attributes and their application in modeling. Agron. J. 107, 1310–1320.
Muchow, R.C., Evensen, C.I., Osgood, R.V., Robertson, M.J., 1997. Yield accumulation in irrigated sugarcane: II. Utilization of intercepted radiation. Agron. J. 89, 646–652.
O'Leary, G.J., 2000. A review of three sugarcane simulation models with respect to their prediction of sucrose yield. Field Crops Res. 68, 97–111.
Ojeda, J.J., Volenec, J.J., Brouder, S.M., Caviglia, O.P., Agnusdei, M.G., 2017. Evaluation of Agricultural Production Systems Simulator as yield predictor of Panicum virgatum and Miscanthus x giganteus in several US environments. GCB Bioenergy 9, 796–816.
Richardson, C.W., Wright, D.A., 1984. WGEN: A Model for Generating Daily Weather Variables. Ars.
Singels, A., Jones, M., Marin, F., Ruane, A., Thorburn, P., 2014. Predicting climate change impacts on sugarcane production at sites in Australia, Brazil and South Africa using the Canegro model. Sugar Tech 16, 347–355.
Stokes, C.J., Inman-Bamber, N.G., Everingham, Y., Sexton, J., 2016. Measuring and modelling CO2 effects on sugarcane. Environ. Model. Softw. 78, 68–78.
Taylor, K.E., Stouffer, R.J., Meehl, G.A., 2011. An overview of CMIP5 and the experiment design. Bull. Am. Meteorol. Soc. 93, 485–498.
Wang, J., Wang, E.L., Luo, Q.Y., Kirby, M., 2009. Modelling the sensitivity of wheat growth and water balance to climate change in Southeast Australia. Clim. Change 96, 79–96.
Wang, B., Liu, D.L., Asseng, S., Macadam, I., Yu, Q., 2015. Impact of climate change on wheat flowering time in eastern Australia. Agric. For. Meteorol. 209, 11–21.
Webster, A.J., Thorburn, P.J., Roebeling, P.C., Horan, H.L., Biggs, J.S., 2009. The expected impact of climate change on nitrogen losses from wet tropical sugarcane production in the Great Barrier Reef region. Mar. Freshw. Res. 60, 1159–1164.
Yang, Y.M., Liu, D.L., Anwar, M.R., O'Leary, G., Macadam, I., Yang, Y.H., 2016. Water use efficiency and crop water balance of rainfed wheat in a semi-arid environment: sensitivity of future changes to projected climate changes and soil type. Theor. Appl. Climatol. 123, 565–579.
Zhang, X., Peng, L., Lin, Z., 2008. Progress on the projections of future climate change with various emission scenarios. Adv. Earth Sci. 23, 174–185.
Zhang, X.-C., 2005. Spatial downscaling of global climate model output for site-specific assessment of crop production and soil erosion. Agric. For. Meteorol. 135, 215–229.
Zhang, X., 2007. A comparison of explicit and implicit spatial downscaling of GCM output for soil erosion and crop production assessments. Clim. Change 84, 337–363.
Zhu, Q., Lowe, E.A., Wei, Y.A., Barnes, D., 2007. Industrial symbiosis in China: a case study of the Guitang Group. J. Ind. Ecol. 11, 31–42.
Zu, Q., Mi, C., Liu, D.L., He, L., Kuang, Z., Fang, Q., Ramp, D., Li, L., Wang, B., Chen, Y., 2018. Spatio-temporal distribution of sugarcane potential yields and yield gaps in Southern China. Eur. J. Agron. 92, 72–83.